Ground Support 2026 - D Cumming-Potvin & J Wesseloo (eds.)
© 2026 Australian Centre for Geomechanics, Perth
doi:10.36487/ACG_repo/2625_25

Advances in probabilistic support design using discrete fracture networks

Audrey Goulet [a,*], Matthew Heinsen Egan [b], Johan Wesseloo [b]

[a] *Australian Centre for Geomechanics, The University of Western Australia, Canada*

[b] *Australian Centre for Geomechanics, The University of Western Australia, Australia*

Abstract

Ground support design in underground excavations is fundamentally influenced by the anisotropic and discontinuous nature of rock masses. This paper presents some recent advances in probabilistic ground support design using discrete fracture network (DFN) modelling. The methodology integrates calibrated DFNs, block identification, stability assessment, and probabilistic risk evaluation to quantify both the likelihood of block occurrence and the probability of block failure. The paper outlines a practical workflow for generating representative DFN models from structural mapping and borehole data, including calibration procedures for fracture orientation, size, and intensity. Thousands of DFN realisations are used to identify tetrahedral blocks around realistic excavation geometries and assess their stability under varying reinforcement and surface support configurations. The approach explicitly captures the influence of rock mass fabric on block formation, support demand, and failure probability, providing a more realistic basis for support design than traditional deterministic methods. The results demonstrate how DFN-based analyses can be used to evaluate support performance probabilistically, compare alternative support standards, and estimate the frequency and magnitude of potentially unstable blocks. The methodology provides a practical framework for moving from deterministic support design towards risk-informed and probabilistic decision-making in underground mining.

Keywords: *discrete fracture network, probabilistic design, ground support, block stability, rock mass fabric, risk assessment*

1 Introduction

The anisotropic and complex nature of rock masses are something which all rock engineers are familiar and deal with on a daily basis. Ironically though, the anisotropic and complex nature of rock masses are not captured well and often ignored in our rock mass characterisation and design approaches.

In mining geomechanics, the complexity of a rock mass is often reduced to a single rock mass rating number, generally without considering the orientation dependent nature of the fabric that determines that number (Figure 1). A rock mass rating is often supplemented with joint orientation and the identification of joint sets. Persistence data (joint size and true spacing) is often neglected and the true fabric of the rock mass not evaluated or assessed in design decisions. The importance of persistence data and the ability to capture the fabric of the rock mass is illustrated in Figure 2. The figure shows 2 discrete fracture networks (DFN) with the same distributions of discontinuity orientation but with different fracture discontinuity intensities.

* Corresponding author. Email address: audrey.goulet@uwa.edu.au

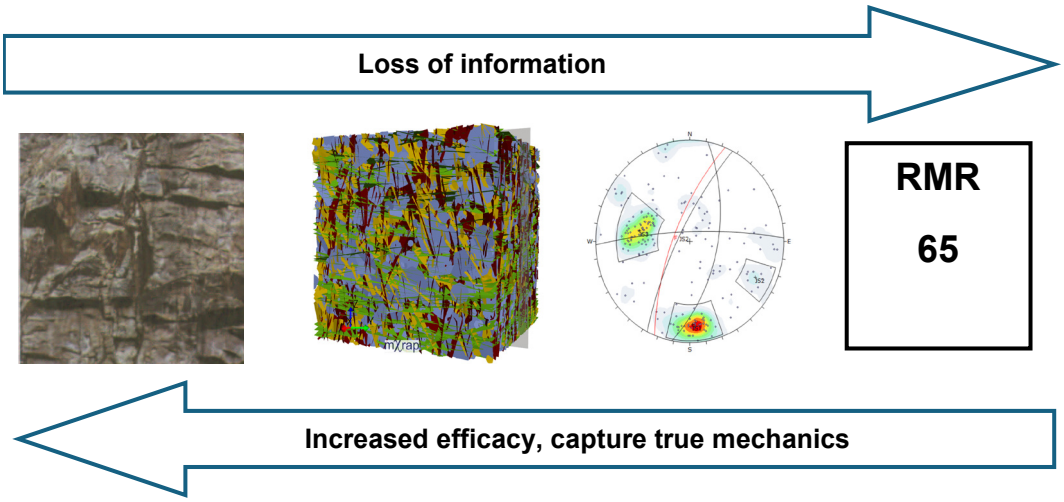


Figure 1 Information loss occurring from complex rock mass to rating systems

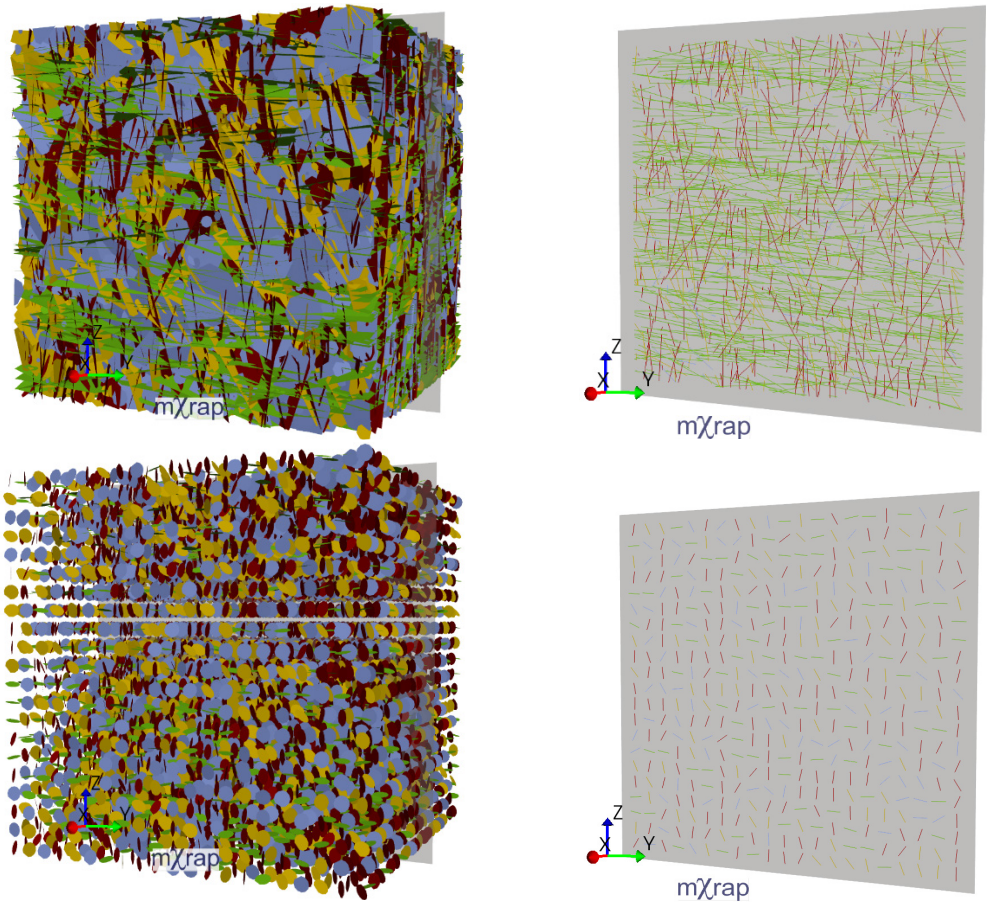


Figure 2 Discrete fracture networks (DFN) and their traces on a vertical plane. The 2 DFNs in this illustration have the same distributions in joint orientation and pole density but with different joint density and persistence

The generation of DFNs to model the fabric of the rock mass in design assessment has become more achievable and practical in recent years allowing more representative analysis and more appropriate design solutions.

The inclusion of representative fracture network models in analysis and design has led to improved results in many applications in open pit and underground mines (e.g. Byrne et al. 2025; Grenon et al. 2026, 2015; Ojeda

et al. 2024; Rogers et al. 2025; St-Hilaire et al. 2025). In this paper, we limit our discussion to the application of DFNs in the analysis of block stability for the purpose of ground support analysis and design. More specifically, this paper focuses on probabilistic stability evaluation.

The ability to capture the fabric of the rock mass enables a rigorous analysis of the probability of block occurrence (PBO).

The probability of a particular block failure occurring is the product of the probability of a block failing and the probability of such a block occurring in the first place, i.e.:

$$Pof_i = Pf[\text{Block}_i|\text{Block}_i \text{ occurs}] \cdot PBO[\text{Block}_i] \quad (1)$$

where:

$Pf[\text{Block}_i|\text{Block}_i \text{ occurs}]$ = the probability of the block failing, given that it occurs

$PBO[\text{Block}_i]$ = the probability of the block occurring.

A lot of attention is generally given to the quantification of the first component, with the second component being neglected or ignored despite it generally having a governing influence on the outcome. Windsor (1999) highlighted that 'proper' design of ground support requires a probabilistic solution that takes into account rock mass fabric and provides for the probability of occurrence of block shapes, sizes, and their stability. Several examples of the applications of such an approach to support design exist (e.g. Grenon & Hadjigeorgiou 2003a, 2003b; Grenon et al. 2017; Hadjigeorgiou & Grenon 2017; Rogers et al. 2017) but it has not yet become common practice. Tyler et al. (2026) recently tested that probabilistic DFN simulations can reproduce large wedges at reduced frequencies and in some instances can generate larger wedges than those from equivalent deterministic assessments at Carapateena mine. Four-way intersections and wide span development drive – both common mine geometries at the site – were compared with the 2 analytical approaches. They highlighted the advantages of probabilistic approaches in balancing safety and economy in their ground support design.

The industry's greatest challenge to do probabilistic analysis is having resources to collect the necessary data (such as the discontinuity persistence), import and calibrate them. For it to become common practise, it needs to be used on a regular basis and fully integrated into geotechnical design, rather than annually for special projects. Improved automation in the data input and DFN calibration processes are well-needed for mine sites to use.

This paper discusses the use of DFNs in support design starting with the topics of DFN generation and calibration, followed by block identification, stability analysis, and probabilistic evaluation.

Several tools for the generation of DFNs are available, with Fracman (WSP 2023) being the most widely known. For this paper, we employed DFN generation and block stability analysis apps developed in mXrap (Harris et al. 2024) – a software platform that provides geotechnical engineers with many data analysis, monitoring and investigation tools. The DFN application in mXrap (Heinsen Egan et al. 2024) is based on Fracture-SG developed by Hadjigeorgiou & Grenon (2000).

2 Generating representative discrete fracture networks

In this paper, we distinguish between a fabric model, a DFN model, and a DFN. The rock mass fabric model determines the shape of the discontinuities, their relative distribution in space, and the interaction of different joint sets (termination, intersection, or coplanarity). Staub et al. (2002) provides a review of different rock mass fabric models.

The DFN model specifies the rock mass fabric model and the set of required input parameters. Many different DFNs can be generated from a single DFN model, each being a legitimate manifestation of the DFN model. Conceptually, a DFN model is a 3D statistical model that captures the spatial variability of the discontinuity fabric of the rock mass. A DFN is therefore not supposed to represent the *exact* discontinuities in an excavation – but to *statistically* represent the rock mass *fabric*.

Many software packages have the capability of generating a fracture network. With any of these software, the generation of DFNs is easy. The generation of a DFN representative of the rock mass is, however, more onerous and requires systematic data collection and calibration of the DFN model. The three-dimensional (3D) nature of the rock mass fabric is not fully captured in the measured parameters and the input parameters capturing the 3D discontinuity intensity cannot directly be measured, hence the necessity for calibration of the DFN model. Calibration of DFN models is an important component of their use as uncalibrated DFN models could be misleading and consequently the interpretation of results challenging or erroneous. Cocha & Shirani Faradonbeh (2026) realised a comparative analysis of calibrated and non-calibrated DFN methods as input for kinematic analysis through 600 iterations for both analyses. For a design criterion of Factor of Safety (FoS) = 1.5, roughly 20% of wedges from the calibrated DFN model have FoS ≤ 1.5, compared with about 40% from the non-calibrated model. In addition, the apex heights also differed from the non-calibrated model (35% less than 1 m) to the calibrated model (<10% less than 1 m). This underscores the significance of calibration for blocks stability assessment from probabilistic analyses.

2.1 Structural data collection

The type of data that needs to be collected refers to orientation, intensity, size and terminations. Multiple characterisation methods allow geotechnical engineers to collect such data. Sewnun et al. (2022) reviewed the structural data collection methods for DFN generation. Two basic approaches are via boreholes core (core logging and geophysical tools in holes) and traditional or digital mapping of exposures. To generate a calibrated DFN model, all the data types must be recorded in sufficient quality, quantity, spatial coverage, in a systematic way and be unbiased.

As mentioned by Sewnun et al. (2022), current structural mining databases are well suited regarding orientation data, but lack proper size and intensity data, which is a critical component of a calibrated and representative DFN model.

Since persistence data was seldom used previously, it is understandable that few mine databases contain persistence and spacing data of sufficient quality and quantity for the DFN calibration process. This lack of persistence data is the industry's greatest challenge in the effective use of DFNs. Sewnun et al. (2022) emphasised that the development of machine learning techniques for gathering structural data is crucial for the use of DFN technology in mines, but there has not been significant progress made since the publication of their paper. In the meantime, it is still possible to generate DFNs but without proper calibration.

2.2 Fabric model selection

To ensure a representative DFN model, a representative fabric model must be selected. Many fabric models require knowledge about discontinuity termination, or discontinuity location distribution. Two discontinuity terminations can be observed in the field: termination in the rock or in another discontinuity. The choice of the DFN model could be guided by the specific joint set configuration and trace terminations observed in the rock mass, which vary from one joint set to another. Currently, the data quality and parameter availability from datasets generally available in industry do not support the use of any DFN model more sophisticated than the simple Baecher model (Baecher & Lanney 1978; Baecher et al. 1977). In this paper, we limit ourselves to the use of the Baecher model.

2.3 Discrete fracture network generation

Once the appropriate fabric model is selected, the required input parameters of the DFN model must be defined. These input parameters are obtained from the calibration process seeded with estimates based on the measured data.

Input parameters for the Baecher model, for each joint set, are:

- Fracture orientation: described by the mean orientation and Fisher-K (akin to standard deviation for the normal distribution).

- Fracture size: in the Baecher model, this is described as the distribution of the disk diameter.
- Fracture intensity: P_{32}, a fracture intensity measure, which corresponds to the sum of fracture area per unit volume, describing the overall 3D fracture density (Dershowitz & Herda 1992).

Is it crucial to understand that fracture size and trace length are distinct terms. Fracture size cannot be directly measured; it is an interpretation of two-dimensional observation data to 3D data. Trace length data act as a footprint for 3D discontinuities as they intersect sampling planes. There is a relationship between the joint diameters and sampled trace lengths which depends on the relative orientation of the excavation surface and the joints, the dimensions of the excavation surface, and the relative location of the sampling line on the excavation surface.

If the rock mass includes randomly oriented structures, a random set can also be included in the DFN inputs. These randomly oriented structures still need to be described by their size and intensity. For randomly oriented structures, the spacing of the set is the same in all directions.

Before calibration, the DFN model parameters are first estimated using the following methods:

- Orientation parameters (mean orientation and Fisher-K): these parameters are directly derived from data, using the methods described in Fisher (1953).
- Mean diameter: a first estimate of the mean diameter can be taken as 0.4-times the mean trace length (Villaescusa & Brown 1992).
- P_{32}: the first estimates of P_{32} are most commonly derived from P_{10} along boreholes and scanlines. A theoretical relationship between P_{32} and P_{10} was developed by Wang (2005).

The relationship between P_{32} and P_{10} can be expressed as:

$$P_{32} = C_{13} \cdot P_{10} \tag{2}$$

C_{13} is dependent on the Fisher-K value and the orientation difference between the borehole/scanline and the mean orientation normal of the joint set, ρ (Table 1).

Table 1 C_{13} for different values of Fisher-K values and the orientation difference, ρ

ρ	Fisher-K									
	0.1	1	2	5	10	50	100	200	500	∞*
0	0.5	0.53	0.62	0.79	0.9	0.98	0.99	0.99	1	1
5	0.5	0.53	0.62	0.79	0.89	0.97	0.98	0.99	0.99	1
10	0.5	0.53	0.61	0.78	0.88	0.96	0.97	0.98	0.98	0.98
20	0.5	0.53	0.59	0.75	0.84	0.91	0.92	0.93	0.93	0.94
30	0.5	0.52	0.56	0.68	0.77	0.84	0.85	0.85	0.85	0.87
40	0.5	0.51	0.54	0.62	0.67	0.74	0.75	0.75	0.75	0.77
50	0.5	0.51	0.51	0.54	0.57	0.62	0.62	0.63	0.63	0.64
60	0.5	0.49	0.48	0.47	0.45	0.47	0.48	0.48	0.48	0.5
70	0.5	0.48	0.45	0.39	0.34	0.32	0.32	0.32	0.32	0.34
80	0.5	0.48	0.44	0.34	0.26	0.18	0.16	0.16	0.16	0.17
90	0.5	0.48	0.44	0.33	0.24	0.11	0.08	0.06	0.04	0

*cos(ρ)

2.4 Calibrating process

To avoid boundary effects, DFNs are generated for a larger volume than the one studied. We include an anulus around the study volume equal in thickness to 3-times the mean joint diameter. Joint centres are sampled within this extended volume, then the joints are clipped to the studied volume.

Once DFN parameters have been created, they need to be calibrated. Calibration involves adjusting the statistical model (DFN model) to the actual data sampled. This calibration process is made by artificially sampling DFNs in the same way the structural data were collected. That allows the same biases to apply for the collected data and the sampled DFN data. Due to that calibration process, it is of crucial importance to have information about the orientation and dimension of surveys. This applies to all structural data sources: borehole, scanline, window mapping, drift mapping, etc.

2.4.1 Data and discrete fracture network sampling

For the boreholes, this means that the same orientation and same relative length is used when artificially sampling the DFNs. For scanlines, the same length and orientation is used. The dimension of the excavation and the relative location of the scanline in the excavation also needs to be considered as this impacts the visibility of trace lengths longer than the excavation size. The importance of this metadata is not always recognised, therefore the data is not always recorded. If this information is unavailable, then we assume that the excavation is 5 m high and that the scanline is taken on the wall 1 m above floor.

Figure 3 shows an example of sampling a DFN using a borehole and a scanline for all joint sets. DFN sampling provides a distribution of dip, dip direction, trace length, and spacing for each joint set. As the DFN generation is a stochastic process, some DFNs may be very different from the mapped data even if they are following the same statistical distribution. To account for this variability, the calibration process can sample several DFNs to provide representative distributions for the parameters.

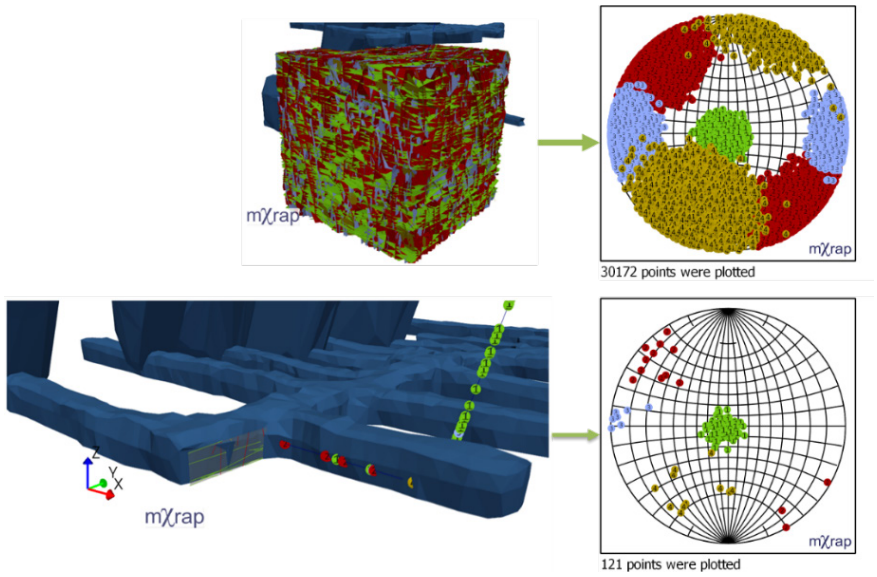


Figure 3 Sampled discrete fracture network the same orientation and direction as the structural data was gathered for a scanline and a borehole

These sampled distributions for each joint set are then compared to the actual data using the 2-sample Kolmogorov-Smirnov (KS) test or Chi-squared test to validate that the data are from the same continuous distribution and have statistically similar means. The KS test usually performs better for small data sets than the Chi-square test. The Chi-square test is meant to test the probability of independence of a distribution of data. The larger the sample size, the more reliable the results.

2.4.2 Iterative process

First, the orientation parameters are calibrated. The mean orientations for each joint set are compared between the mapped data and the sampled DFNs. The orientation comparison is made with the normal vectors so that the 3D orientation is properly compared. It is also possible to visually compare the density of fracture orientations on a stereonet. If the orientation sampled from the DFNs does not fit the mapped data then the sets might not be following a normal 3D distribution, as it is assumed for the Fisher-K distribution.

Second, the mean diameter needs to be calibrated. The trace lengths from the data are compared to the trace lengths sampled from DFN. Both trace lengths distributions are compared down to the minimum trace length mapped only, to avoid the truncation bias. The geometry of the excavation (5 m high per default, horizontal, oriented as the scanline) being take into consideration while sampling the trace lengths of the DFN, the censoring bias applies similarly for the data and the sampled DFN. Note that if mean trace length is near the excavation dimensions (relative to the orientation of the sets), it is an indicator that the dimensions of the joints are larger than what is recorded. Such instances are a warning flag that the number of visible ends should be investigated to confirm the sampling bias. It is necessary to investigate the influence of much *larger* joints on the forming of blocks. To assess which mean diameter inputs are needed to obtain certain sampled trace length means, multiple DFNs are generated with different mean diameter inputs. A best-fit curve is calculated between the mean diameter inputs and the mean sampled trace lengths. From that curve, we can determine the optimal mean diameter inputs which would correspond to the mean trace lengths from the mapped data. DFNs with the optimal mean diameter are then generated and the mean sampled trace lengths from the DFNs are compared with the mean trace lengths from the data using the KS test and Chi-squared test.

Third, the P_{32} can be calibrated by investigating the normal joint spacing. To assess which P_{32} input is needed to obtain a certain sampled normal joint spacing, multiple DFNs are generated with different P_{32} parameters. A curve of best-fit is calculated between the P_{32} inputs and the resulting normal joint spacings. From that curve, one can determine the optimal P_{32} input corresponding to the *sampled* normal joint spacing from data. Afterwards, the normal joint spacing from data is compared the ones sampled from the DFN.

Fourth, if the mean diameter parameters are changed, then the P_{32} parameter calibration should be re-verified. The normal joint spacing depends on both the mean diameter and the P_{32}, so it is possible that a change in mean diameter will produce a difference in the sampled normal joint spacing. The DFN model is considered calibrated when the DFN-sampled data statistically correlates with the structural field data. The full iterative process of the calibration is illustrated in Figure 4.

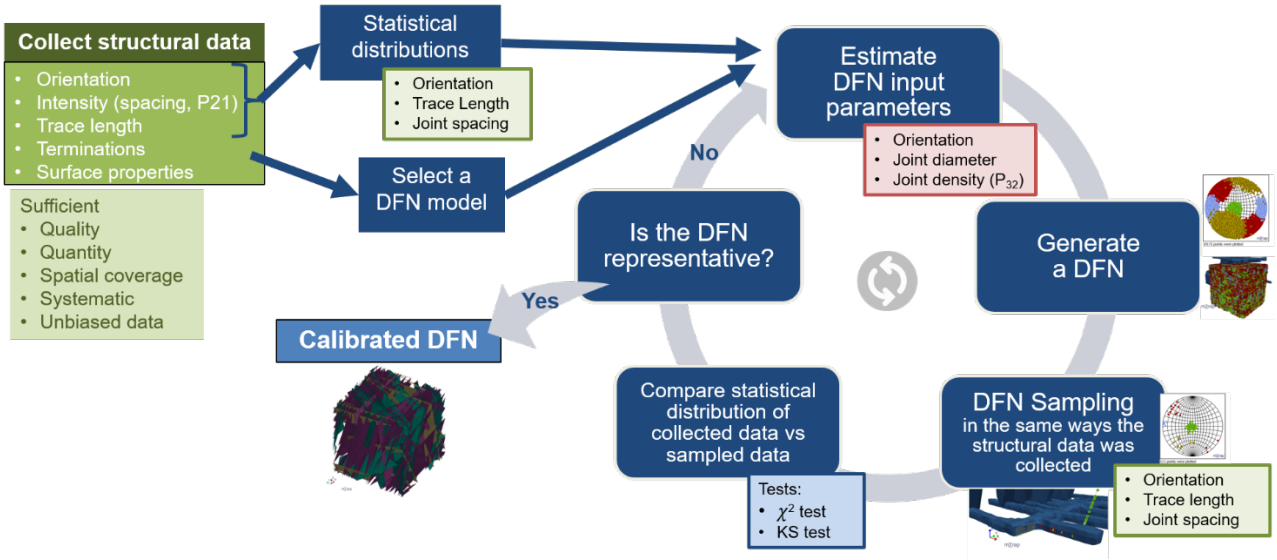


Figure 4 Discrete fracture network calibration process in mXrap

3 Block identification and stability assessment process

Once a calibrated DFN model is obtained, it can be used to investigate the blocks generated around an excavation. With a calibrated model, many separate DFNs can be generated. Over large volumes, the analysed behaviour of a DFN will tend towards the mean, with wide scatter manifesting at smaller scales. To capture the true variation of block formation at drive scale many DFNs need to be generated and their block formation analysed.

The analysis is performed with an iterative process where DFNs are generated and analysed until enough removable blocks have been found to enable further probabilistic analysis. The iterative process is illustrated in the flowchart presented in Figure 5. This process results in a set of recorded blocks and their properties available for stability analysis.

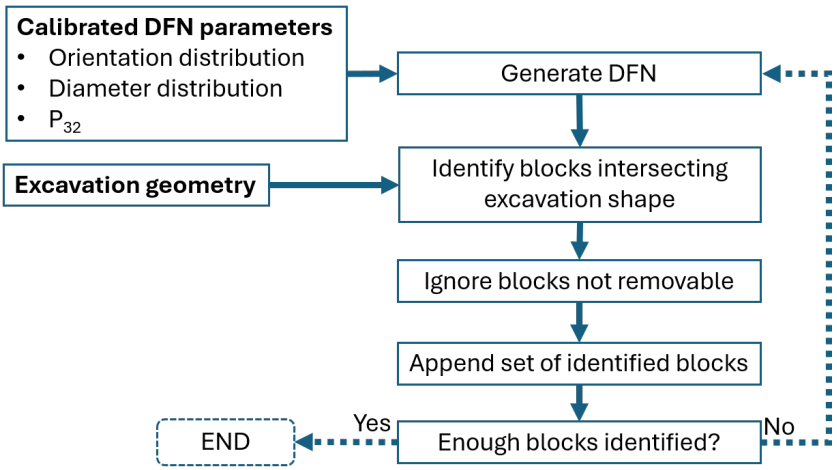


Figure 5 Process of block finding

Stability of the blocks is analysed following the process flow illustrated in Figure 6. Many small blocks are formed. These blocks are of no consequence due to their very small size and the fact that such blocks will be removed during blasting. These blocks are filtered out if their volume, weight, or depth falls below user specified thresholds. The stability of the remaining blocks is then analysed.

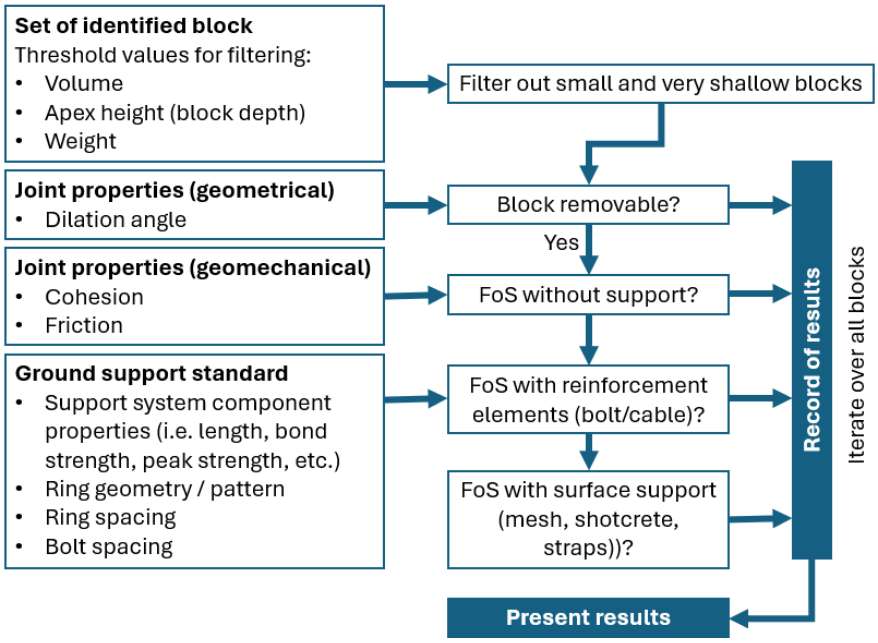


Figure 6 Process of block stability analysis of identified blocks

Firstly, each block is tested for removability, taking the dilation angle into account (see Section 3.2). Standard stability analysis is then performed on all removable blocks to assess their stability without the effect of ground support.

User-specified ground support systems provide the ring layout and ring spacing of reinforcement elements as well as tensile resistance properties. The relative location of the reinforcing tendons and the calculated block are used to analyse the stability of the block with the effect of the reinforcement tendons.

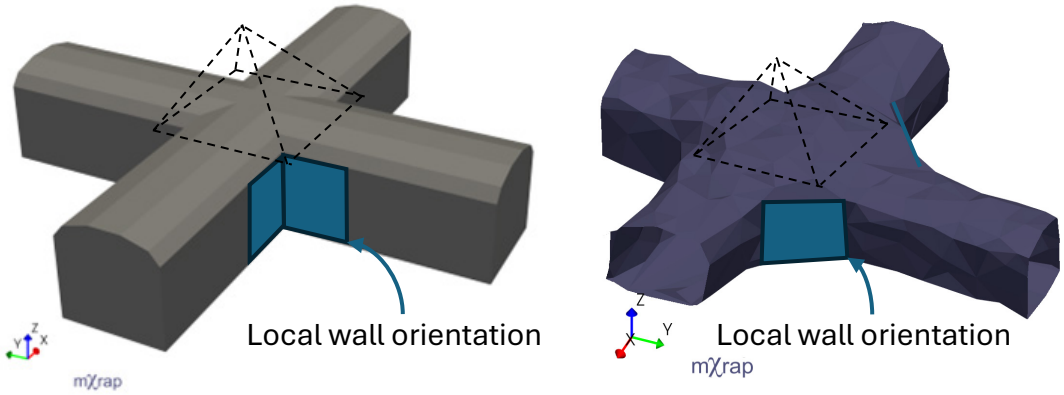
Blocks that are unstable with ground support tendons applied are also tested for stability against a passive surface support.

These steps are discussed in more detail in the following sections.

3.1 Block identification

For assessing ground support requirements, it is necessary to identify the blocks forming between different joints in the DFN and the excavation geometry. A detailed 3D representation of the excavation geometry is preferred, as it is more representative of the field conditions. Figure 7 compares the design shape and as-built geometry of a four-way intersection. The perfect 90° bullnoses of the design shape result in a smaller span, which in turn underestimates the number of blocks and the size of the largest block that can be produced. More importantly, the wall orientation is not the same and therefore a different combination of joints may combine with the excavation surface to form unstable blocks.

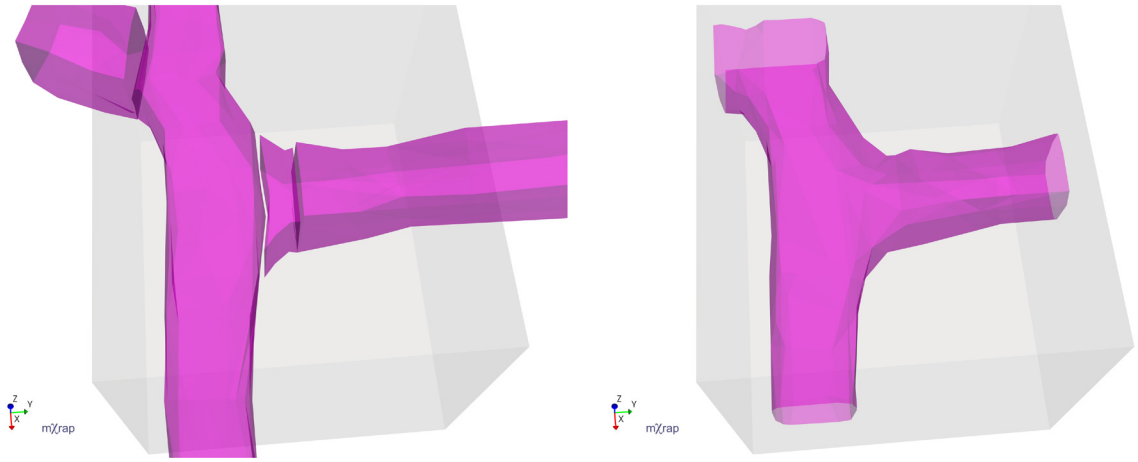
Durham et al. (2023) compared tetrahedral block formation from a DFN using a surveyed excavation geometry, simplified versions of the surveyed geometry, and the original planned geometry. They found that the wedges formed were significantly different when using the most simplified geometry or the planned geometry, noting that “over-simplification can result in non-representative wedge assessment and misleading information” (Durham et al. 2023).



(a) (b)

Figure 7 (a) Designed intersection versus (b) 3D surveyed intersection. For illustration purposes, a pentahedral block with a square footprint was added

Importing excavation shapes from different software can create challenges for managing mesh quality. The block finding process is impacted by mesh quality problems such as self-intersections, internal surfaces, or holes. To enable intersection analysis and block identification, the mesh needs to be oriented and valid. The simplest approach to all these problems is to remesh the geometry of interest to comply with these requirements. Figure 8 shows an example of remeshing a poor-quality input mesh: the intersection is formed by separate volumes which are detached in some areas and intersecting in others, the remeshing result is a single combined volume without self-intersections.

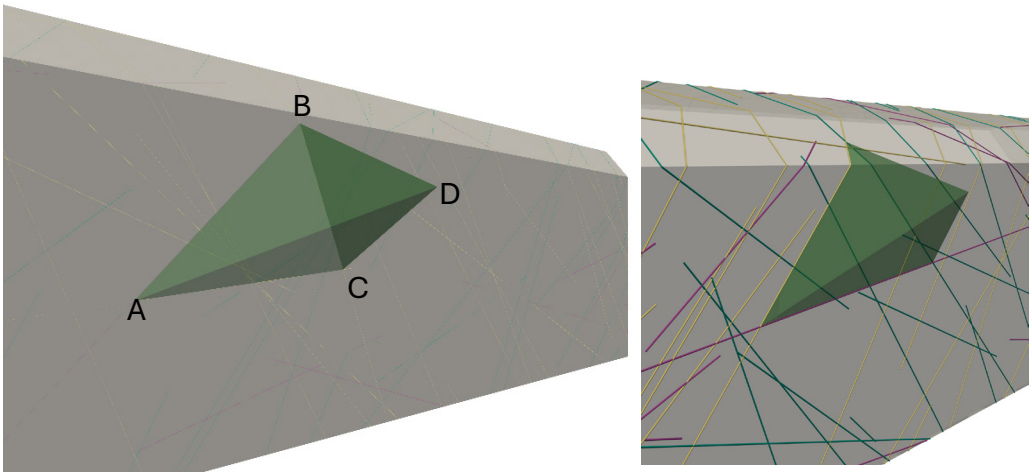


(a) (b)

Figure 8 (a) A poor-quality input mesh; (b) The result of remeshing

The block finding process begins by finding the intersection of the joints and the surface of the mesh, effectively the trace lines of the joints on the excavation. These trace lines are plotted as shown in Figure 9, which may give users a visual method to judge whether the DFN realisations are realistic compared to their experience of the rock mass. A tetrahedral block's base on the excavation will be 3 trace lines which are connected in a loop, so the next step in the block finding is to search the trace lines to find any such loops. When a loop is found, we then need to check if the block is completely formed or if there is a rock bridge. A loop of 3 joints A, B, and C (Figure 9a) has 3 corners on the excavation surface formed by the intersections of AB, BC, and CA. The intersection of 2 joints forms a line segment in 3D space. If we follow the line segments for AB, BC, and CA away from the excavation surface, then we can check if all 3 of those segments intersect. If they do, then a complete tetrahedral block is formed, and the intersection of the 3 segments at point D is the apex of the tetrahedron.

While the blocks are tetrahedral insofar as they are created from 3 joints, the shape of the excavation makes the final block shape more complex. The excavation volume needs to be removed from the simple tetrahedron, so that the base of the block curves according to the shape of the excavation, as shown in Figure 9b.



(a) (b)

Figure 9 Illustration of finding identifying tetrahedral blocks. (a) From a loop of 3 joints; (b) Removing the excavation volume.

Enough DFNs must be generated to have a statistically representative sample of blocks. We can assess this by investigating the stability of the block weight statistics (median, mean, percentile, etc.) in relation to the

number of DFNs generated. An example is shown in Figure 10, we can see that the mean and median weights have stabilised by the time we reached 500 DFNs, though the maximum weight continues to increase even as we approach 3,000 DFNs. Generating additional DFNs, beyond the amount required to stabilise the block weight median, can provide for a better distribution of blocks around our excavation surface. We recommend aiming for the stability of the higher percentile (e.g. 97 percentile) to have statistical representations of the biggest blocks. This is useful for probabilistic analysis of ground support requirements in different areas of the excavation. It is not important to generate the absolute maximum block size with the Monte Carlo approach since this value can be calculated deterministically and the probability distribution of the infrequent block sizes can be estimated, as discussed in Section 4.4.

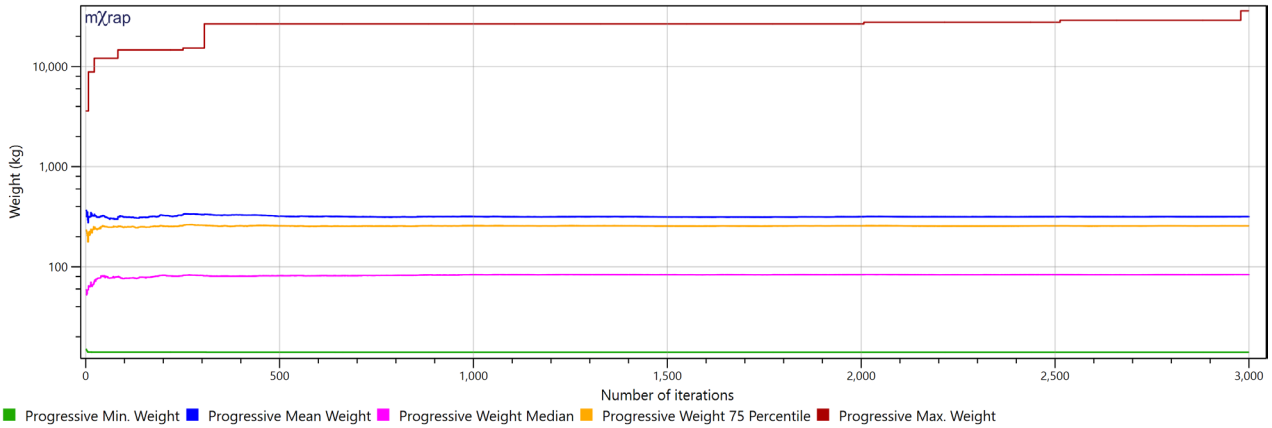


Figure 10 Block weight statistics in relation to number of discrete fracture networks generated

3.2 Stability analysis

The nature of the fracture generation model and the block finding process results in some blocks which are mathematically correct, but either not realistic or not of practical concern and best filtered from further analysis.

Many small blocks are found on the surface of the excavation, which would be removed in the initial blasting. To exclude these blocks there are filters for block volume, block weight, and apex height (the depth of the tetrahedron apex from the excavation surface).

Because the fracture generation model creates perfectly planar joints there can be very thin blocks, either flat triangles or thin spikes, which are mathematically removable and unstable. An example is shown in Figure 11.

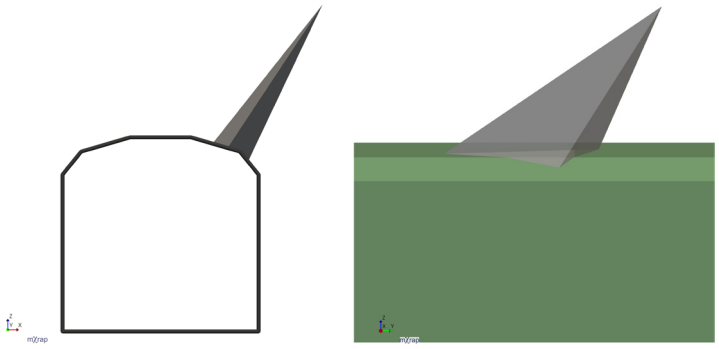


Figure 11 Example of a thin wedge formed in a discrete fracture network

The effect of cohesion and friction strength for the joints forming these blocks is often not enough to stabilise larger blocks with unrealistic aspect ratios. For unrealistic blocks that are falling directly down, the joint strength properties will not have any effect on the FoS calculation. From experience, we know that blocks of this type are inherently stable and a clamping force is often enacted to generate enough frictional resistance to ensure stability of these blocks. Most blocks of this type are, however, eliminated with the addition of a dilation angle to the removability test.

Conceptually the dilation angle is the minimum angle required between the block's direction of movement and the surface of the joint, due to the joint's roughness. Users can specify a dilation angle for each joint set. In Figure 12, the blue line shows the surface of the joint that a block would slide along, and the green line shows the direction of movement with a dilation angle of 5˚.

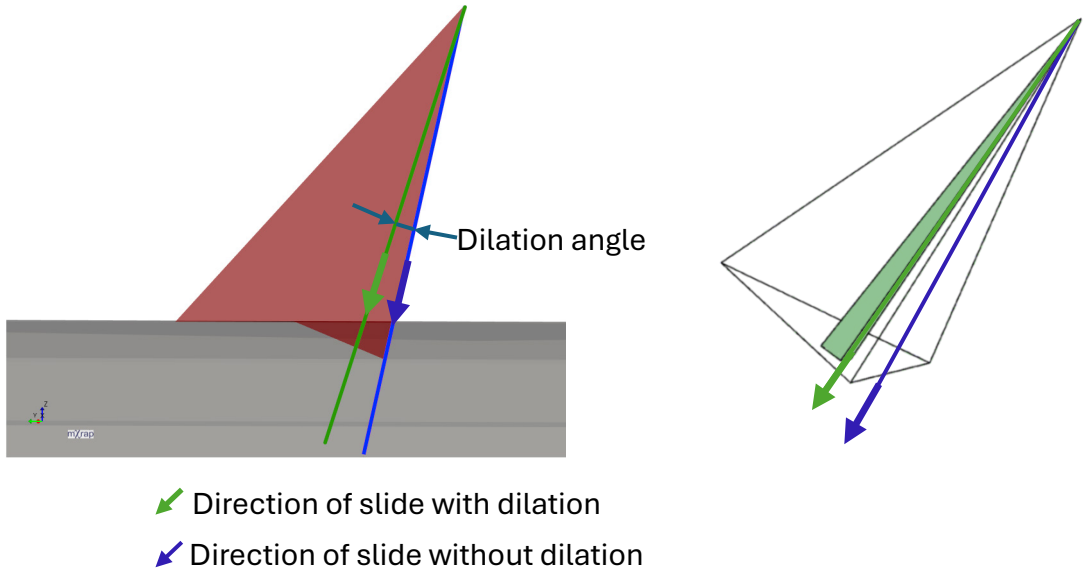


Figure 12 Direction of sliding influenced by the dilation angle

The direction of movement is determined using the joint pyramid method of Goodman & Shi (1985). As we only have tetrahedral blocks, it is simple to consider the pyramid formed by the joint surfaces. The line of movement is the closest line to the direction of gravity that lies within the pyramid. Figure 12 above shows a wireframe of the joint pyramid calculated for the thin wedge that was shown in Figure 11. The line of movement is shown extending beyond the joint pyramid; in this case the block is sliding on the intersection of 2 joints. When dilation angles are specified, a new pyramid is created by adjusting each joint surface according to the angle of dilation. The smaller internal pyramid shown in Figure 11 results from a dilation angle of 4° for each joint. If we increased the dilation angle to 5°, then the adjusted pyramid would close completely, and the block would be excluded from analysis.

Block stability is influenced by the joint properties, intersecting bolts, and surface support. For intersecting bolts an effective capacity is calculated based on the anchored length of the bolt (m), the bolt's bond strength (t/m), and the bolt's peak strength (t). The effective capacity is the lesser of the peak strength and the bond strength multiplied by the anchored length. If a section of the bolt extends out of the block in the same direction as the block's direction of movement, e.g. the bottom section of the rightmost bolt in Figure 13, then that section of the bolt will not contribute any capacity. This simplifies the analysis, but in a way that makes the analysis more conservative.

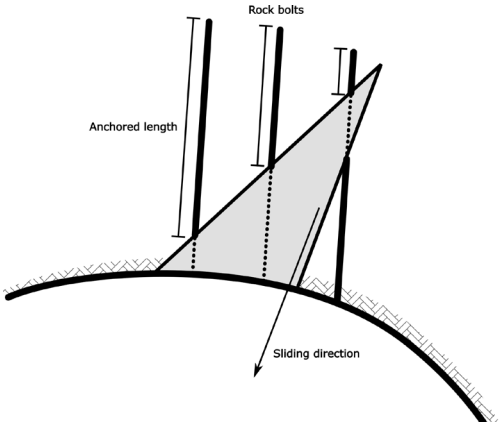


Figure 13 Definition sketch for stability analysis with rockbolts

The FoS based on the joint strength properties and bolts is calculated following the formulae used by Grenon & Hadjigeorgiou (2003a). If the FoS is less than 1, then we also consider surface support for the block. Surface support is implemented as a fixed weight capacity for any blocks that are covered by the surface support. If these blocks are also intersected by bolts, then the effective FoS is the higher of the FoS using only the bolts or the FoS using only the surface support, i.e. the bolts and surface support do not both contribute to the support for a single block.

4 Decision-making and communication of results

There are multiple tools in mXrap that allow the user to capture the geometry of the blocks regarding the excavation, the ground support relationship with the blocks, the stability of the blocks, and the current and future ground support performance. All of these can be used for validation purposes, communication and decision-making.

4.1 Blocks analysis

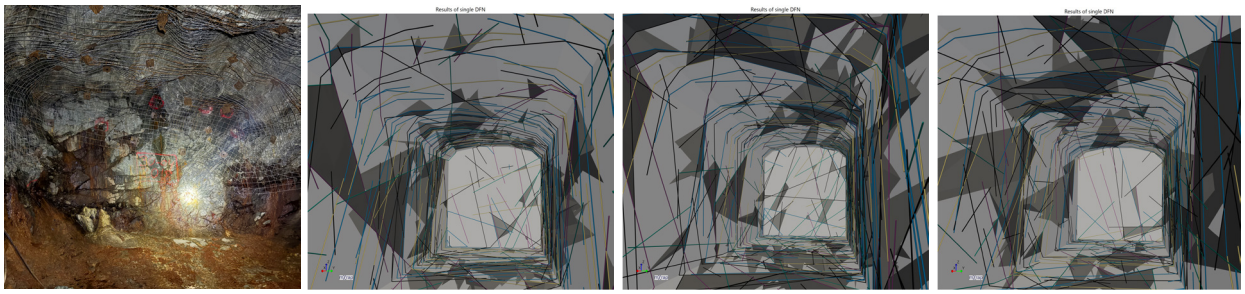
The 3D visualisations of the blocks and discontinuity traces allow the user to have sanity checks of the DFN generated blocks. It is important that the blocks created by the DFN are somewhat similar to underground observations. It is possible to compare different elements from the DFN to underground observations:

- volume of failed wedges
- overall geometry of the blocks/wedges generated
- excavation profile to DFN tunnel profile (example in Figure 14)
- joint traces on excavations (example in Figure 15).



(a) (b) (c)

Figure 14 Comparison of tetrahedral blocks versus complex blocks for an excavation with the same discrete fracture network inputs. (a) 1 iteration – tethrahedral blocks; (b) Photo of tunnel profile; (c) 1 iteration – complex blocks



(a) (b) (c) (d)

Figure 15 Comparison of joint traces on a face versus traces of 3 different discrete fracture network iterations (DFN). (a) Photo of face; (b) DFN iteration A; (c) DFN iteration B; (d) DFN iteration C

4.2 Ground support standard stability analysis

DFNs allow us to probabilistically assess ground support standard performance. The way the stability analysis works was described in Section 3.2. For this calculation to happen correctly, the mechanical properties of the joint surface, the properties of each ground support element and the geometrical placement of each ground support element must be specified. Geometrical placement can be specified automatically or manually from a 2D view of the tunnel profile, providing the position and angle of each element.

The joint surface properties, ground support reinforcement elements, and surface support each have a different impact on block stability, as shown in Figure 16. In this case, the joint properties mainly affect the stability of the blocks that are less than 1 tonne. The bolts have a huge impact on the stability of all blocks, while the surface support affects the blocks under a fixed weight threshold.

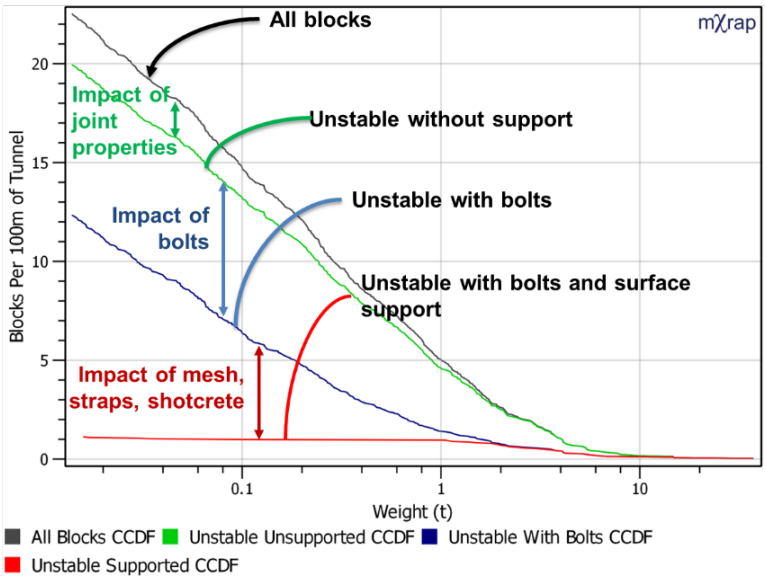


Figure 16 Complementary cumulative distribution function (CCDF) of the number of generated blocks per 100 m of tunnel by weight considering different elements of the ground support

The 3D visualisation also allows us to assess the anchoring depth of the ground support (Figure 17a) for each block, while a 2D profile allows us to assess the distribution of anchoring depths for each reinforcement element in profile (Figure 17b). High failure rates of bolts in the 2D view indicate that more support is needed in that area of the profile. Conversely, a bolt taking no charge might be replaced, or the spacing may be increased.

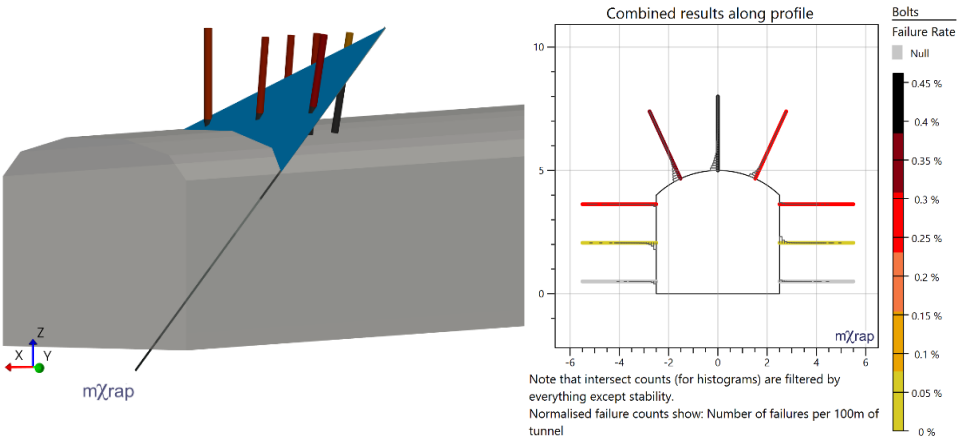


Figure 17 Visualisation of anchoring depth in (a) 3D and (b) along a 2D profile

4.3 Varying ground support standards

Having identified the blocks forming between discontinuities and the excavation surfaces, it is a fairly easy process to test the stabilising performance of different ground support systems against the set of identified blocks and their relative location in the excavation and with respect to the ground support. Figure 18 shows the gain in stability of doubling the number of bolts, going from a pattern of 2 × 2 m (Pattern 1) to a pattern or 1 × 1 m (Pattern 3), along with the middle-case (Pattern 2; 1.5 × 1.5 m).

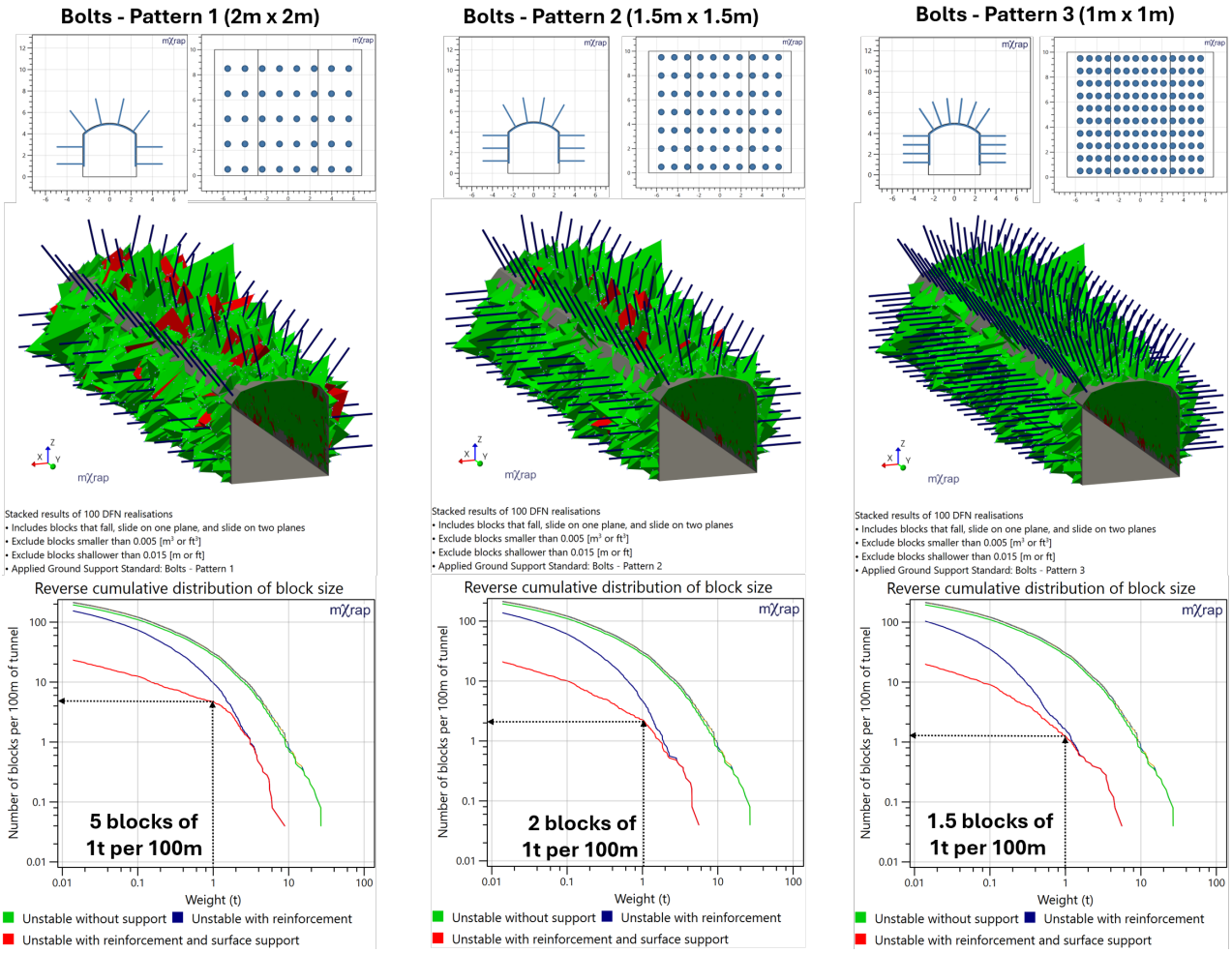


Figure 18 Comparison of 2 ground support standards performance for the same blocks

4.4 Probabilistic risk evaluation

At the scale of ground support evaluation, the difference between each DFN is large compared to the excavation size and the spacing of support units. As a result, many DFNs need to be generated for each calibrated DFN model and the support evaluated probabilistically. With every extra generated DFN, the set of generated blocks increase, and with that the size of the largest generated block. However, the probability of generating a block larger than the largest block previously generated, diminishes with every extra DFN. On the other hand, the size of the largest possible block can be estimated deterministically. After performing many iterations, a gap will remain between the largest generated block and the largest possible block.

The probability of occurrence of very large and infrequently occurring blocks can be determined by obtaining a probability distribution representative of the obtained block sizes with an upper limit equal to the deterministically obtained maximum block size. For this we use the standard beta distribution. The minimum value is taken simply as the smallest generated block size after applying the filtering as described in Section 3. The fitted beta distribution for larger block sizes is not sensitive to the minimum value.

Figure 19 shows the distribution of expected block sizes and indicate that the largest possible block is about 46 tonnes. Per definition, the probability of exceeding this block size is zero. A block greater than 5 tonnes is expected to occur, on average, once every 100 m, whilst block sizes exceeding 20 tonnes are expected to occur at a rate of 1 every 5 km. Small blocks are expected to occur very frequently. The consequence of the failure of different size blocks in terms of safety and economics is of course different, with smaller sized blocks easily stabilised by ground support.

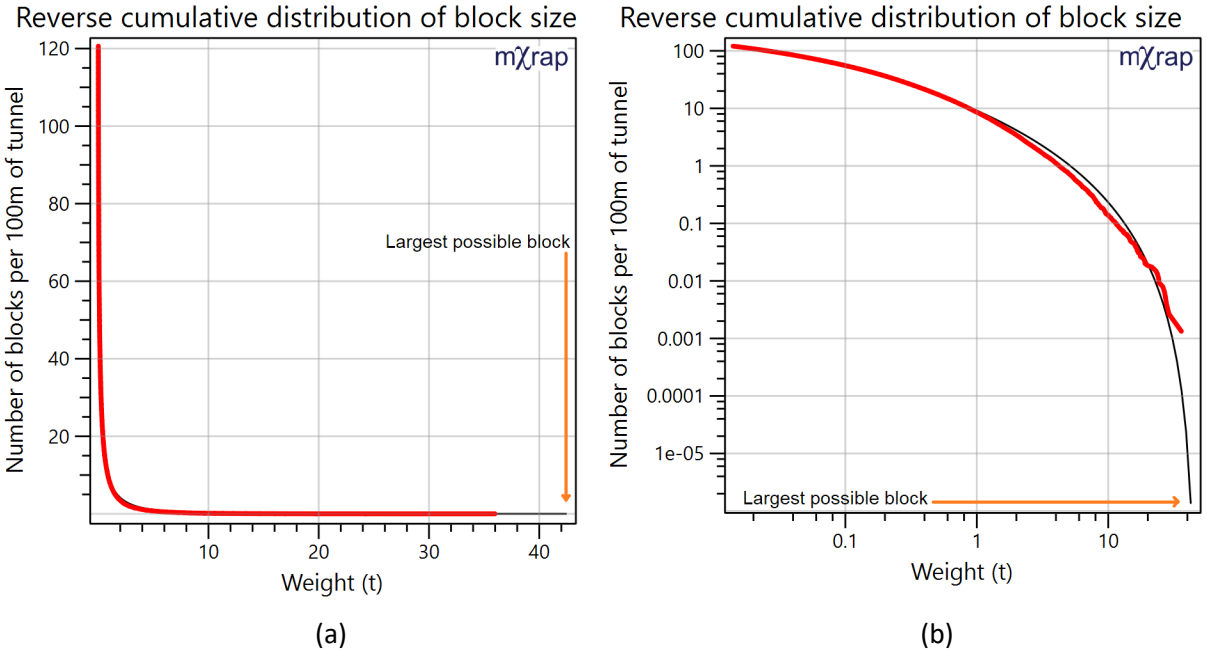


Figure 19 Distribution of generated block sizes with fitted Beta distribution with (a) block weight on normal scale and (b) block weight on logarithmic scale

The relative gain or loss of benefit between different support systems can be assessed very easily and the change from current support systems to a different support system easily justified. A more difficult question, however, is determining the values for probability of failure for different block sizes that could be regarded as acceptable. A strong argument can be made that one need not design for the largest possible block as the probability of it occurring is negligible. The cutoff design probability of failure is ultimately a risk-based decision.

The most significant economic consequences are from the cost of rehabilitation of the damaged section (depth of failure, volume failed, length of damage) and the loss of production due to inaccessibility during rehabilitation (Joughin et al. 2020). The safety risk evaluation considers the probability of excessive damage, the exposure of personnel to rockfall and the coincidence probability in evaluating the overall probability of

fatality for different numbers of people. Joughin et al. (2020) proposed a methodology for developing a risk model to enable the back calculation of the required probability of failure to achieve prescribed risk acceptance levels.

The approach described by Joughin et al. (2020) is not easy to implement and further development towards probabilistic design acceptance criteria is required. Future work needs to connect the tolerable risk criteria defined in corporate procedure to probabilistic design such as the ones we are aiming for using DFNs.

5 Complex blocks

This paper focuses on tetrahedral blocks. We have also developed a system that can identify complex block shapes formed by the DFN and excavation (see Figure 14c), based on the procedure described by (Yu et al. 2009). Compared to the tetrahedral block identification, this more general method finds many more blocks. However, it takes far more computational time and has far higher memory usage, which limits the maximum number of fractures that can be analysed. Furthermore, the stability analysis of these complex block formations is significantly more complicated due to the blocks interacting with each other, and due to the presence of non-convex blocks. While the focus on tetrahedral blocks is a common simplification (for example Grenon et al. 2026, Durham et al. 2023, UnWedge [Rocscience Inc. 2023]), it will not be sufficiently representative for all domains.

6 Conclusion

This paper demonstrates the application of DFN modelling as a practical framework for probabilistic ground support design in underground excavations.

The successful application of DFNs depends on the development of calibrated fracture network models. Calibration requires high-quality orientation data which is generally available, and reliable fracture intensity data – the most significant limitation in many current mining databases.

The probabilistic workflow presented combines DFN generation, block identification, stability analysis, and support assessment. Repeated DFN realisations allow the natural variability of block formation to be quantified and provide estimates of both block occurrence and block stability. Support performance can be evaluated in terms of the full distribution of potential block sizes. A successful application of probabilistic wedges design at a mine site can be found in Tyler et al. (2026).

The methodology enables direct comparison of alternative support standards. The use of realistic excavation geometries, combined with explicit modelling of reinforcement and surface support interactions, further improves the representativeness of the analysis. While the present work focuses on tetrahedral block formations, the study also highlights the future potential of more advanced algorithms capable of assessing complex block geometries.

Finally, DFN-based support design represents an important step toward risk-based geotechnical engineering. By linking the PBO with the probability of instability, the approach establishes a foundation for future support design methodologies based on acceptable risk criteria rather than deterministic factors of safety alone. Further work is required to establish industry-wide probabilistic design acceptance criteria and to integrate economic and safety consequences directly into support design decisions.

Acknowledgement

This study was funded by the Ground Support System Optimisation Phase 3 (GSSO 3) research project at the Australian Centre for Geomechanics, The University of Western Australia. Major project sponsors were: 29Metals, Agnico Eagle - LaRonde mine and Canadian Malartic mine, BHP- Nickel West, Evolution, Gold Fields Australia, MMG Limited, Rio Tinto Oyu Tolgoi mine, St Barbara Mines and Vale Sudbury Operations. Minor project sponsors were: DSI Underground (a Sandvik Company), Geobrugg, Jennmar Australia, Normet, Sika.

There have been contributions from many engineers working with sponsoring mines and suppliers, assisting in providing data, participating in fruitful discussions, and providing our team with wisdom and guidance to ensure practical research outcomes would be produced from the GSSO 3 project. Although there are too many of our colleagues from the mining industry to provide names here, we acknowledge this important contribution, and we are very grateful for it.

We also want to express our sincere thanks to the leader of GSSO3, Professor Yves Potvin.

References

Baecher, GB & Lanney, NA 1978, 'Trace length biases in joint surveys', *19th U.S. Symposium on Rock Mechanics*, University of Nevada, Reno, pp. 56–65.

Baecher, GB, Lanney, NA & Einstein, HH 1977, 'Statistical description of rock properties and sampling', *18th U.S. Symposium on Rock Mechanics*, American Rock Mechanics Association, Golden.

Byrne, C, Rogers, S, Stevenson, M, Pothitos, F & Tennant, D 2025, 'Bench design optimisation in a sparsely structured rock mass', in JJ Potter & J Wesseloo (eds), *SSIM 2025: Fourth International Slope Stability in Mining Conference*, Australian Centre for Geomechanics, Perth, https://doi.org/10.36487/ACG_repo/2535_06

Cocha, E & Shirani Faradonbeh, R 2026, 'Probabilistic stability assessment of underground mining structures through discrete fracture network modelling: a case study in Western Australia', *Australian Conference on Rock Mechanics*.

Dershowitz, WS & Herda, HH 1992, 'Interpretation of fracture spacing and intensity', in JR Tillerson & WR Wawersik (eds), *Proceedings of the 33rd U.S. Symposium on Rock Mechanics*, A.A. Balkema, Rotterdam.

Durham, C, Grenon, M, Karampinos, E & Dorion, JF 2023, 'Numerical Investigation on the Impact of Drift Geometry Representation on the Assessment of Wedge Formation Using DFN Modelling in Underground Hard Rock Mines', *Proceedings of the 57th U.S. Rock Mechanics/Geomechanics Symposium*, American Rock Mechanics Association, Eaton, https://doi.org/10.56952/arma-2023-0739

Fisher, RA 1953, 'Dispersion on a sphere', P*roceedings of the Royal Society of London. A. Mathematical and Physical Sciences*, vol. 217, no. 1130, pp. 295–305, https://doi.org/10.1098/rspa.1953.0064

Goodman, RE & Shi, G 1985, *Block Theory and Its Application to Rock Engineering*, Prentice-Hall, New Jersey.

Grenon, M & Hadjigeorgiou, J 2003a, 'Drift reinforcement design based on discontinuity network modelling', *International Journal of Rock Mechanics and Mining Sciences*, vol. 40, no. 6, pp. 833–845, https://doi.org/10.1016/S1365-1609(03)00044-3

Grenon, M & Hadjigeorgiou, J 2003b, 'Open stope stability using 3D joint networks', *Rock Mechanics and Rock Engineering*, vol. 36, no. 3, pp. 183–208, https://doi.org/10.1007/s00603-002-0042-0

Grenon, M, Karampinos, E, Durham, C, Liao, JK, Grenon, JB, Dorion, JF & Tuleau, J 2026, 'Integrated risk-based design approach for wedge hazard in underground mining drifts', *Canadian Geotechnical Journal*, vol. 63, pp. 1–20, https://doi.org/10.1139/cgj-2025-0245

Grenon, M, Landry, A, Hadjigeorgiou, J & Lajoie, PL 2015, 'Contribution to drift design using discrete fracture network modelling at the Éléonore Mine in Canada', in Y Potvin (ed.), *Design Methods 2015: Proceedings of the International Seminar on Design Methods in Underground Mining*, Australian Centre for Geomechanics, Perth, pp. 339–350, https://doi.org/10.36487/ACG_rep/1511_20_Grenon

Grenon, M, Landry, A, Hadjigeorgiou, J & Lajoie, PL 2017, 'Discrete fracture network based drift stability at the Éléonore mine', *Mining Technology*, vol. 126, no. 1, pp. 22–33, https://doi.org/10.1080/14749009.2016.1199296

Hadjigeorgiou, J & Grenon, M 2000, 'Geomechanical analysis using simulated 3D natural joint networks', in TN Michalakopoulos & GN Panagiotou (eds), *Mine Planning and Equipment Selection 2000*, Routledge, London.

Hadjigeorgiou, J & Grenon, M 2017, 'Drift reinforcement design based on Discrete Fracture Network (DFN) modeling', in X-T Feng (ed.), *Rock Mechanics and Engineering*, CRC Press, Boca Raton.

Harris, PC, Heinsen Egan, M, Niedzielski, LG & Cumming-Potvin, D 2024, *mXrap*, version 6.0, computer software, Australian Centre for Geomechanics, Perth, https://mxrap.com/

Heinsen Egan, M, Sewnun, D, Goulet, A, Wei Ho, C & Wesseloo, J 2024, *Discrete Fracture Network Suite*, computer software, Australian Centre for Geomechanics, Perth.

Joughin, WC, Wesseloo, J, Mbenza, J, Mpunzi, P & Sewnun, D 2020, 'A risk-based approach to ground support design', in Y Potvin & J Hadjigeorgiou (eds), *Ground support for underground mines*, Australian Centre for Geomechanics, Perth. pp. 399–433.

Ojeda, P, Fogel, Y, Roy, J, Valerio, C & Rogers, S 2024, 'Probabilistic three-dimensional kinematic analysis to improve design reliability of complex underground excavations', in P Andrieux & D Cumming-Potvin (eds), *Deep Mining 2024: Proceedings of the 10th International Conference on Deep and High Stress Mining*, Australian Centre for Geomechanics, Perth, pp. 1103–1114, https://doi.org/10.36487/ACG_repo/2465_71

Rocscience Inc. 2023, *UnWedge*, computer software, Toronto, https://www.rocscience.com/software/unwedge

Rogers, S, Byrne, C, Fogel, Y, Ojeda, P, Pere, V & Correia, C 2025, 'De-risking a Pilbara iron ore pit slope design through a stochastic structural stability assessment', in JJ Potter & J Wesseloo (eds), *SSIM 2025: Fourth International Slope Stability in Mining Conference*, Australian Centre for Geomechanics, Perth, https://doi.org/10.36487/ACG_repo/2535_39

Rogers, SF, Bewick, RP, Brzovic, A & Gaudreau, D 2017, 'Integrating photogrammetry and discrete fracture network modelling for improved conditional simulation of underground wedge stability', *Deep Mining 2017: Proceedings of the Eighth International*

Conference on Deep and High Stress Mining, Australian Centre for Geomechanics, Perth, https://doi.org/10.36487/ACG_rep/1704_40_Rogers

Sewnun, D, Wesseloo, J & Heinsen Egan, M 2022, 'A review of structural data collection methodologies for discrete fracture network generation', in Y Potvin (ed.), *Caving 2022: Proceedings of the Fifth International Conference on Block and Sublevel Caving*, Australian Centre for Geomechanics, Perth, pp. 1047–1060, https://doi.org/10.36487/ACG_repo/2205_72

St-Hilaire, P, Grenon, M & Wilson, B 2025, 'Optimising ramp design using discrete fracture network cost-based analysis', in JJ Potter & J Wesseloo (eds), *SSIM 2025: Fourth International Slope Stability in Mining Conference*, Australian Centre for Geomechanics, Perth, https://doi.org/10.36487/ACG_repo/2535_40

Staub, I, Fredriksson, A & Outters, N 2002, *Strategy for a Rock Mechanics Site Descriptive Model Development and Testing of the Theoretical Approach*, Svensk Kärnbränslehantering AB, Solna.

Tyler, A, Goulet, A, Heinsen Egan, M, Wesseloo, J, Potvin, Y & Chester, C 2026, 'Probabilistic vs deterministic wedge formation methods', in D Cumming-Potvin & J Wesseloo (eds), *Ground Support 2026: 11th International Conference on Ground Support in Mining*, Australian Centre for Geomechanics, Perth, https://doi.org/10.36487/ACG_repo/2625_26

Villaescusa, E & Brown, ET 1992, 'Maximum likelihood estimation of joint size from trace length measurements', *Rock Mechanics and Rock Engineering*, vol. 25, no. 2, pp. 67–87, https://doi.org/10.1007/bf01040513

Wang, X 2005, *Stereological Interpretation of Rock Fracture Traces on Borehole Walls and Other Cylindrical Surfaces*, Virginia Polytechnic Institute and State University, Blacksburg.

Windsor, CR 1999, 'Systematic design of reinforcement and support schemes for excavations in jointed rock', in E Villaescusa, CR Windsor & AG Thompson (eds), *International Symposium on Ground Support and Reinforcement Practice in Mining*, Balkema, Kalgoorlie, pp. 35–58.

WSP 2023, *FracMan*, computer software, FracMan Technology Group, Montreal, https://www.wsp.com/en-us/services/fracman/

Yu, Q, Ohnishi, Y, Xue, G & Chen, D 2009, 'A generalized procedure to identify three-dimensional rock blocks around complex excavations', *International Journal for Numerical and Analytical Methods in Geomechanics*, vol. 33, no. 3, pp. 355–375, https://doi.org/10.1002/nag.720